Prolonged Charge-Separated States of Starburst Tetra(diphenylaminofluoreno)[60]fullerene Adducts upon Photoexcitation

Mohamed E. El-Khouly,[†,‡] Robinson Anandakathir,[§] Osamu Ito,[†] and Long Y. Chiang*[,§]

Institute of Multidisciplinary Research for Advanced Materials, Tohoku University, Katahira, Aoba-ku, Sendai 980-8577, Japan, Department of Chemistry, Faculty of Education, Tanta University, Kafr El-Sheikh, Egypt, and Department of Chemistry, University of Massachusetts Lowell, Lowell, Massachusetts 01854

Received: March 19, 2007; In Final Form: May 15, 2007

Construction of starburst $C_{60}(>DPAF\text{-}C_9)_4$ pentads was coupled with the use of highly fluorescent diphenylaminofluorene-C_9 (DPAF-C_9) addends as donor components in conjunction with the fullerene acceptor during single-photon excitation processes. High quantum yields (Φ_{CS}) of charge-separation processes in the range 0.83−0.90 for $C_{60}(>DPAF\text{-}C_9)_n$ ($n = 1$, 2, or 4) were obtained in the formation of $C_{60}^{\bullet-}(>DPAF^{\bullet+}\text{-}C_9)(>DPAF\text{-}C_9)_{n-1}$ transient states. The lifetime of the radical ion-pairs (τ_{RIP}) was found to be 900 ns for starburst $C_{60}(>DPAF\text{-}C_9)_4$ (**3**) samples, which is 6-fold longer than that of the linear analogue $C_{60}(>DPAF\text{-}C_9)$ (**1**), with a ca. 2 times increase of the charge-separation rate (k_{CS}) compared to that of **1**. These data implied the important role of sterically hindered DPAF-C_9 pendants arranged in a starburst-like environment that encapsulates the central C_{60} core on extending the τ_{RIP}. We interpreted the phenomena by the occurrence of intramolecular migration or exchange of electron or positive charge among multiple DPAF-C_9 pendants of $C_{60}^{\bullet-}(>DPAF^{\bullet+}\text{-}C_9)(>DPAF\text{-}C_9)_{n-1}$, which gives an increased rate in charge generation and delayed charge recombination.

Introduction

Intramolecular electron- or energy-transfer phenomena from the donor moiety to the C_{60} moiety upon single-photon excitation of C_{60}−donor assemblies have been extensively reviewed.[1] The phenomena lead to the formation of the corresponding charge-separated $(C_{60}>)^{\bullet-}$−$(donor)^{\bullet+}$ or triplet C_{60} ($^3C_{60}^*>$) excited transient states. Utilization of these transient states to enhance their potential applications in the area of molecular electronic devices,[2] photovoltaic cells,[3] and photodynamic sensitizers[4] has been proposed. Closely related to the single-photon excitation process, the occurrence of simultaneous two-photon excitation processes for several C_{60}−donor conjugated dyad molecules has also been demonstrated.[5,6] An example was given by $C_{60}(>DPAF\text{-}C_2)$, where a two-photon absorptive (2PA) chromophore [7-(1,2-dihydro-1,2-methano[60]fullerene-61-carbonyl)-9,9-diethyl-2-diphenylaminofluorene (DPAF-C_2)] was used as the donor component of the C_{60}−keto−donor assembly.[5] A number of related chromophore dyads [$C_{60}(>DPAF\text{-}C_n$), where C_n represents variable alkyl groups attached on the fluorene ring] exhibit significant photoresponsive nonlinear activities that were attributed to large 2PA cross-section enhancement. Enhancement of cross-section values was correlated to the increase of electronic interactions and molecular polarization between donor and acceptor moieties, which were proposed to serve as potential optical power limiting materials.[7] Optical properties are highly dependent upon the variation of donor−acceptor structures and the tendency of the resulting C_{60}−keto−donor assemblies to aggregate. Structural alteration of the $C_{60}(>DPAF\text{-}C_2)$ dyad by replacing two ethyl groups with two sterically hindered 3,5,5-trimethylhexyl (C_9) groups to form $C_{60}(>DPAF\text{-}C_9)$ was found to largely increase the optical properties.[8] Subsequent structural modification that introduced multiple DPAF-C_9 chromophore arms on one C_{60} cage, to effect molecular cage separation and minimize physical aggregation, resulted in a further increase of the nonlinear photonic efficiency.[9] Apparently, the design of a starburst C_{60}−keto−DPAF assembly with a C_{60} cage as the central core resembles its encapsulation by four bulky DPAF-C_9 arms in the structure of $C_{60}(>DPAF\text{-}C_n)_4$ that led to a surprising multiphoton absorption (MPA) enhancement and an optical limiting effect.[9] Therefore, it is of interest to investigate the complementary photoinduced intramolecular electron-transfer effect of starburst $C_{60}(>DPAF\text{-}C_9)_n$ structures containing multiple photoresponsive chromophore pendants in comparison with that of the linear $C_{60}(>DPAF\text{-}C_9)$ dyad.

Here, we report photoinduced transient states of $C_{60}(>DPAF\text{-}C_9)_n$ ($n = 1$, 2, or 4), as shown in Figure 1, in either toluene or dimethylformamide (DMF) using DPAF-C_9 pendants acting as antenna components for light harvesting at visible wavelengths. The structural design of C_{60}−keto−DPAF assemblies includes a close linkage of the photoactive DPAF-C_n chromophore arm to the fullerene cage at a short separation distance of roughly 2.0 Å via a keto bridging group. The motif allows through-space intramolecular communication between C_{60} and DPAF-C_n moieties to be effective. This donor−acceptor interaction was reasoned for facile electron delocalization and molecular polarization of $C_{60}(>DPAF\text{-}C_9)$.[8] Subsequent intersystem energy-crossing occurs on a time scale of 1.3 ns, based on the detection of the T_1-T_n transient absorption of $^3C_{60}^*>$ at 700−750 nm with a lifetime of ~33 μs in toluene.[10]

Competitive intramolecular photoinduced electron-transfer processes from the $^1DPAF^*\text{-}C_2$ moiety to the $C_{60}>$ moiety of this type of donor−acceptor assembly can be achieved in polar solvents. Accordingly, the charge-separation quantum yield of

* To whom correspondence should be addressed. E-mail: Long_Chiang@uml.edu.
† Tohoku University.
‡ Tanta University.
§ University of Massachusetts Lowell.

10.1021/jp072193j CCC: $37.00
Published on Web 07/11/2007

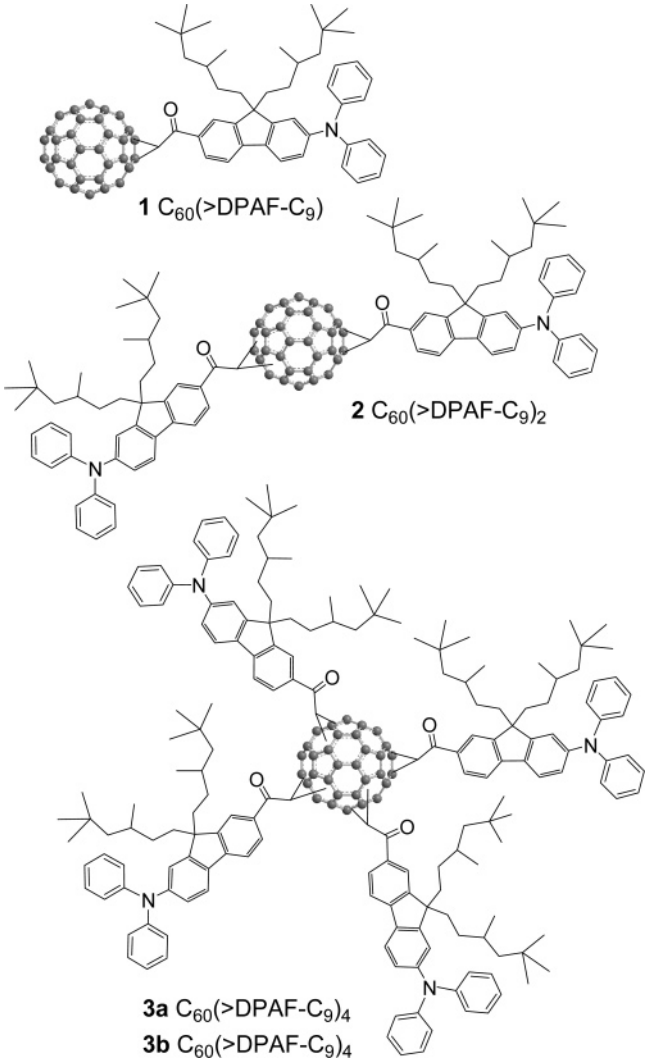

Figure 1. Molecular structures of $C_{60}(>DPAF\text{-}C_9)_n$ (**1** for $n = 1$, **2** for $n = 2$, and **3** for $n = 4$) showing the resemblance of C_{60} cage encapsulation by DPAF-C_9 arms when n increases. Structures **3a** and **3b** were isolated from chromatographic bands at $R_f = 0.5$ and 0.25, respectively, by TLC (SiO_2, hexane/toluene (2:3) as the eluent), giving similar photophysical characteristics.

$C_{60}^{\bullet-}(>DPAF^{\bullet+}\text{-}C_2)$ derived from $C_{60}(>{}^1DPAF^*\text{-}C_2)$ may reach 0.96 in PhCN, with a long-lived charge-separated state with a 150 ns lifetime.[10] Similar intramolecular electron-transfer phenomena were also detectable in self-assembled $C_{60}(>DPAF\text{-}EG_n)$, where EG_n is oligo(ethylene glycol), nanostructures in water.[11] Extension from these linear monoadduct structures to the related starburst multiadduct analogous $C_{60}(>DPAF\text{-}C_9)_n$ should allow us to investigate the structural relationship in terms of the molecular branching to photophysics of $C_{60}-DPAF\text{-}C_n$.

Experimental Section

Material Preparations. Preparation of the [60]fullerenyl monoadduct (**1**) and bisadduct (**2**) has previously been described.[8] Synthesis of the [60]fullerenyl tetraadduct $C_{60}(>DPAF\text{-}C_9)_4$ (**3**, C_{60}[methanocarbonyl-7-(9,9-di(3,5,5-trimethylhexyl)-2-diphenylaminofluorene)]$_4$) was carried out by the reaction of finely divided C_{60} and 7-α-bromoacetyl-9,9-di(3,5,5-trimethylhexyl)-2-diphenylaminofluorene (α-BrDPAF-C_9) in the presence of 1,8-diazabicyclo[5.4.0]undec-7-ene (DBU) in anhydrous toluene. All reaction conditions and workup details follow those of the recently reported procedure.[12] Accordingly, compound **3a** was isolated in an orange-brownish chromatographic band ($R_f = 0.5$ using hexane/toluene in a ratio of 2:3 as the eluent) on semipreparative TLC (SiO_2) plates to give an 18% yield, which was used for several photophysical investigations in the present study. Molecular weights of **1**, **2**, and **3a** were clearly confirmed by positive ion matrix-assisted laser desorption ionization mass spectrum (MALDI-MS) using α-cyano-4-hydroxycinnamic acid as the matrix, as shown in Figure 2 panels a−c, respectively. All of these spectra displayed a group of mass peaks with a maximum peak intensity centered at either $m/z = 1345$, 1972, or 3224, and the related isotope peaks indicated a molecular ion mass (MH^+) of **1**, **2**, or **3a**, respectively. The latter two mass ion peaks were followed by a group of mass peaks centered at $m/z = 1346$, which matched that of **1** that has lost exactly one or two CH_2(DPAF-C_9) ($m/z = 626$) subunits from fragmentation of the molecular mass. In the low-mass ion region, several major peaks at $m/z = 612-629$, including the masses of DPAF-C_9 ($m/z = 612$) and CH-(DPAF-C_9) ($m/z = 625$), were observed that revealed facile fragmentation at the bonds immediately next to either the C_{60} or the methano[60]fullerene cage. A relatively simple spectrum pattern in the high-mass region implied good stability of the aromatic keto-diphenylaminofluorene moiety under MALDI-MS measurement conditions. Characteristics of all spectroscopic data, including FT-IR, UV−vis, and ^{1}H NMR spectra, corresponding to DPAF-C_9 and $C_{60}>$ moieties of **1** and **2**, were applied as the analytical reference for the structural identification of **3a**. In addition, a second fraction was isolated at $R_f = 0.25$ in a 7% yield and was assigned as regioisomer **3b** (Supporting Information). No significant quantity of [60]fullerene hexaads or higher adducts were isolable.

Instrumentation. Electrochemical redox potential values were measured using the differential pulse voltammetry (DPV) technique by applying a BAS CV-50W voltammetric analyzer. A platinum disk electrode was used as the working electrode with a platinum wire and a Ag/AgCl electrode serving as the counter and reference electrodes, respectively. All measurements were carried out in DMF containing $(n\text{-}Bu)_4N^+ClO_4^-$ (0.1 M) as a supporting electrolyte at a scan rate of 0.1 V s^{-1}.

Steady-state fluorescence spectra were collected on a Shimadzu RF-5300 PC spectrofluorophotometer equipped with a photomultiplier tube having high sensitivity in the 700−800 nm region. Fluorescence lifetimes were measured by a single-photon counting method using a second harmonic generation (SHG, 400 nm) of a Ti:sapphire laser (Spectra-Physica, Tsunami 3950-L2S, 1.5 ps full-width at half-maximum (fwhm)) and a streakscope (Hamamatsu Photonics) equipped with a polychromator as excitation source and a detector, respectively. Lifetimes were evaluated with the software installed in the equipment. Nanosecond transient absorption measurements in the near-infrared (IR) region were carried out by laser-flash photolysis using an excitation light source of a Nd:YAG laser (Spectra-Physics and Quanta-Ray GCR-130, 6 ns fwhm) operated at 355 nm. Monitoring lights from a pulsed Xe-lamp were detected via a Ge-avalanche photodiode module. Prior to the measurement, the sample solution in a quartz cell (1.0 × 1.0 cm) was deaerated by bubbling argon gas for 20 min.

Results and Discussion

Photophysical Studies in Starburst Tetra(diphenylaminofluoreno)[60]fullerene Adducts. Steady-state UV−vis absorption spectra of $C_{60}(>DPAF\text{-}C_9)_n$ and two comparable model compounds (7-acetyl-9,9-di(3,5,5-trimethylhexyl)-2-diphenylaminofluorene [CH_3(DPAF-C_9)] and $C_{60}>$) in toluene are displayed in Figure 3. Optical absorption of **1** gave two major

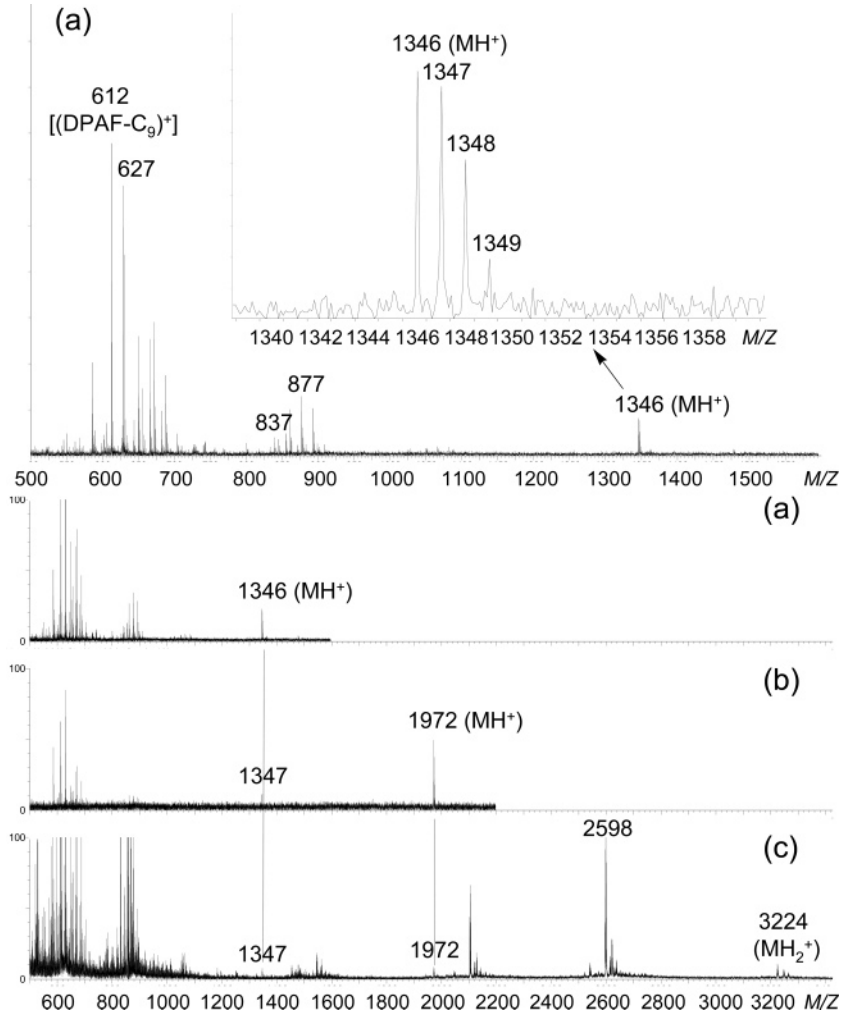

Figure 2. MALDI-TOF mass spectrum of (a) the monoadduct **1** (M^+, $m/z = 1345$), (b) the bisadduct **2** (M^+, $m/z = 1971$), and (c) the tetraadduct **3a** (M^+, $m/z = 3222$) using α-cyano-4-hydroxycinnamic acid as the matrix.

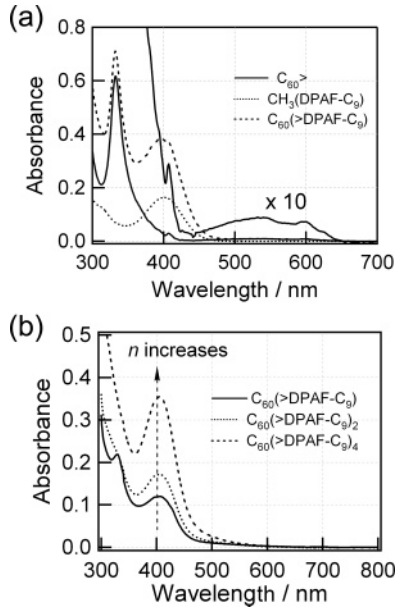

Figure 3. Steady-state absorption spectra of (a) $C_{60}>$, CH_3(DPAF-C_9), and **1** and (b) $C_{60}(>$DPAF-$C_9)_n$ as **1** ($n = 1$), **2** ($n = 2$), and **3a** ($n = 4$) in a concentration of 5×10^{-6} M in toluene.

bands centered at 320 and 405 nm. The former band approximately matched that of model compound $C_{60}>$, which mainly contained an optically active fullerene cage moiety that allowed us to correlate this band to absorption characteristics of a $C_{60}>$ cage containing 58 conjugated π-electrons. The latter band fits the main optical absorption of CH_3(DPAF-C_9) centered at 299 and 407 nm that is attributed to the visible absorption of the diphenylaminofluorene moiety. Nearly absorptive superimposition of **1** with the combined spectra of two independent chromophores containing either the fullerene cage or the diphenylaminofluorene moiety revealed no ground-state interaction between these two components in toluene. As the number of DPAF-C_9 addends increases to two and four in the structures of **2** and **3a**, respectively, the absorption intensity of the DPAF-C_9 components at 405−407 nm becomes significant and increases to almost 1.4- and 3.0-fold higher than that of **1**, which is roughly consistent with their corresponding compositions.

The photophysical behavior of $C_{60}(>$DPAF-$C_9)_n$ was investigated first by steady-state fluorescence measurements. The fluorescence peaks of ^{1}DPAF*-C_9 of $C_{60}(>$DPAF-$C_9)_n$ in toluene were located between 450 and 460 nm, from which the lowest excited singlet energy of $C_{60}(>{}^1$DPAF*-$C_9)$ was calculated to be 2.74 eV. In benzonitrile, the fluorescence bands of ^{1}DPAF*-C_9 of $C_{60}(>$DPAF-$C_9)_n$ are red-shifted, as compared to those in toluene, at 471, 478, and 508 nm for **1**, **2**, and **3a**, respectively. Such red-shifted emission bands may be attributed to the CT excited state. Despite the nearly exclusive excitation of the ^{1}DPAF*-C_9 moiety (i.e., ∼80%), the $C_{60}>$ fluorescence peak appears at 714 nm, as shown in Figure 4a. The spectral shape and intensity of this fluorescence emission from

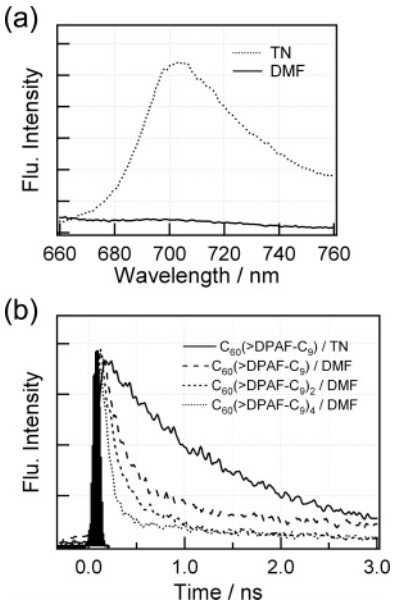

Figure 4. (a) Steady-state fluorescence spectra of **1** (5×10^{-6} M) in either toluene (TN) or DMF and (b) fluorescence decay profiles of $C_{60}(>DPAF\text{-}C_9)_n$ in either TN or DMF in the region of 700−800 nm with $\lambda_{ex} = 400$ nm.

$^1C_{60}^*(>DPAF\text{-}C_9)$ in toluene were found to bear a close resemblance to those of the reference model $C_{60}>$.[14] Thus, these observations correlated to the energy-transfer from $^1DPAF^*\text{-}C_9$ to the lowest excited singlet energy of $^1C_{60}^*(>DPAF\text{-}C_9)$, which was estimated to be 1.75 eV.

Contrarily, the use of DMF as the solvent led to nearly full quenching of the $^1C_{60}^*(>DPAF\text{-}C_9)$-based fluorescence emission band at 714 nm (Figure 4a) that is indicative of its nearly quantitative consecutive process via the $^1C_{60}^*>$ state. One plausible explanation is the occurrence of intramolecular electron-transfer from a covalently attached DPAF-C_9 pendant to the fullerene cage either before or after the intramolecular energy-transfer process that was facilitated by close contact of these two components. In addition, the high incompatibility of the $C_{60}>$ cage moiety with polar DMF may induce heterogeneous molecular aggregation of **1** in favor of cage−cage interactions that might contribute in part to the solvent-dependent electron-transfer process occurring from DPAF-C_9 to $^1C_{60}^*>$ in the quenching pathway that yields the corresponding charge-polarized intermediate $C_{60}^{\bullet-}(>DPAF^{\bullet+}\text{-}C_9)$.

Fluorescence lifetime measurements track the above considerations in a more quantitative manner to estimate the kinetics of the charge-separation processes. As a reference, the fluorescence decay-time profile of $CH_3(DPAF\text{-}C_9)$ recorded at 400−600 nm exhibited a single-exponential decrease with a lifetime (τ_{f0}) of 3200 ps. Similar decay profiles were also obtained for the samples of **2** and **3a**. Fluorescence lifetimes of the $^1DPAF^*\text{-}C_9$ moiety of $C_{60}(>DPAF\text{-}C_9)_n$ ($n = 2$ or 4) were almost the same as those of $CH_3(DPAF\text{-}C_9)$ in toluene and DMF, suggesting no occurrence of the charge-separation via the route of $C_{60}(>{}^1DPAF^*\text{-}C_9)$ in the time resolution of the present laser pulse (10 ps), although this observation might not always be consistent with the ultrafast process.

With scanning the detection range in the 700−800 nm region, the fluorescence band appeared at 710 nm, which corresponds to the emission of the $^1C_{60}^*>$ moiety of **1** in toluene, as shown in Figure 4a. The time profile of this band displayed single-exponential decay in toluene with a lifetime of 1400 ps, which is nearly the same as the fluorescence lifetime (τ_{f0}) of the $C_{60}>$ reference, suggesting no charge-separation is taking place via the $^1C_{60}^*>$ moiety in toluene. In the case of DMF as a solvent, substantial quenching of the $C_{60}>$ fluorescence lifetimes (τ_f) was detected (Figure 4b) for **1** as compared to the lifetime of the $C_{60}>$ reference. It implied that the event of charge-separation takes place via the $^1C_{60}^*>$ moiety in DMF. Accordingly, two-component fluorescence decays of $^1C_{60}^*>$ were observed (Figure 4b). The major fast-decaying components exhibited τ_f values of 240 ps (81%), 200 ps (87%), and 150 ps (90%) for the samples **1**, **2**, and **3a**, respectively (Table 1). The τ_f values of the second slow-decaying component were found in a similar range to that of $C_{60}>$. The rapid fluorescence decay component could arise from the intramolecular charge-separation event between the $^1C_{60}^*>$ and DPAF-C_9 moieties in the compounds. On the basis of the short τ_f values of $^1C_{60}^*>$ in DMF, quantum yields (Φ_{CS}) of this charge-separation process via $^1C_{60}^*(>DPAF\text{-}C_9)_n$ were evaluated as 0.83, 0.86, and 0.90 for **1**, **2**, and **3a**, respectively, with good photoefficiency and a slightly increased value upon the increasing number of the DPAF-C_9 pendants from **1** to **3a**. Accordingly, the calculated charge-separation rate constants (k_{CS}) were also found to increase by ca. 2.0 in the same trend, going from 3.40×10^9 s^{-1} for **1** to 5.96×10^9 s^{-1} for **3a**.

The charge-separation processes from (DPAF-C_9) to $^1C_{60}^*>$ were supported from the viewpoint of the thermodynamics of the electron-transfer processes. The value of electrochemical redox potentials of $C_{60}(>DPAF\text{-}C_9)_n$ is a crucial factor for the determination and evaluation of the free-energy of electron-transfer processes between $C_{60}>$ and DPAF-C_9 moieties. Redox potential values were measured in the same solvent (DMF) using the DPV technique. In this polar solvent, the DPV profiles indicated that the first oxidation potential of the DPAF-C_9 donor moiety is positioned at 660, 672, and 676 mV vs Ag/Ag^+ for the samples of **1**, **2**, and **3a**, respectively. These are in a similar range, indicating that there is little differentiation in value among the monoadduct and multiadducts. The first reduction potential of the $C_{60}>$ acceptor moiety was −796 mV vs Ag/Ag^+, which is in the same potential range for **1**, **2**, and **3a**. The energy levels ($-\Delta G_{CS}$) of the radical ion pairs in toluene and DMF were evaluated using the Weller-type approach with the application of these redox potential values, the center-to-center distance, and the dielectric constant.[13] Consequently, the driving forces of the charge-separation ($-\Delta G_{CS}$) process in DMF were calculated as 0.35, 0.34, and 0.33 eV (Table 1) for **1**, **2**, and **3a**, respectively, which suggests an exothermic charge-separation process for moving one electron from the DPAF-C_9 moiety to the $^1C_{60}^*>$ moiety in these donor−acceptor conjugates to form the corresponding $C_{60}^{\bullet-}(>DPAF^{\bullet+}\text{-}C_9)(>DPAF\text{-}C_9)_{n-1}$. In nonpolar toluene, on the other hand, the positive ΔG_{CS} values for all $C_{60}(>DPAF\text{-}C_9)_n$ conjugates suggest an unfavorable endothermic charge-separation process via $^1C_{60}^*>$. The opposite signs of free energy values in different solvents imply a strong solvent-dependency of the intramolecular electron-transfer processes of $C_{60}(>DPAF\text{-}C_9)_n$ systems, which are favorable only in polar solvents.

Moreover, the charge-separation processes were supported by further investigation of the molecular geometry and electronic structure of the studied compounds. Computational calculations of $C_{60}(>DPAF\text{-}C_9)_n$ conjugates were performed by using density functional theory (DFT) methods at the B3LYP/3-21G level. Fully optimized structures of $C_{60}(>DPAF\text{-}C_9)_n$ were obtained for the highest occupied molecular orbital (HOMO) and the lowest unoccupied molecular orbital (LUMO), as shown in Supporting Information. The radii of ion radicals of DPAF-C_9

TABLE 1: Free-Energy Changes (ΔG_{CS}), Fluorescence Lifetimes of $^1C_{60}^*$> (τ_f), Rate Constants (k_{CS}) and Quantum Yields (Φ_{CS}) of the Charge-Separation Process, Rates Constants of Charge-Recombination (k_{CR}), and Lifetimes of Radical Ion-Pairs (τ_{RIP}) of C_{60}(>DPAF-C_9)$_n$ in Toluene (TN) and DMF[a]

compounds	solvent	$-\Delta G_{CR}$ / eV	$-\Delta G_{CS}$ / eV	τ_f / ns	k_{CS} / s^{-1}	Φ_{CS}	k_{CR} / s^{-1}	τ_{RIP} / ns
1	TN	1.94	−0.21	1.52				
	DMF	1.40	0.35	0.24 (81%) 1.90 (19%)	3.40×10^9	0.83	6.60×10^6	150
2	TN	1.95	−0.20	1.45				
	DMF	1.41	0.34	0.20 (87%) 2.34 (13%)	4.30×10^9	0.86	1.60×10^6	620
3a	TN	1.96	−0.19	1.50				
	DMF	1.42	0.33	0.15 (90%) 1.70 (10%)	5.96×10^9	0.90	1.10×10^6	900

[a] The driving forces for ΔG_{CR} and ΔG_{CS} were calculated by the equations[13] $-\Delta G_{CR} = e(E_{ox} - E_{red}) - \Delta G_S$ and $-\Delta G_{CS} = \Delta E_{00} - (-\Delta G_{CR})$, where ΔE_{00} is the energy of the 0−0 transition (1.75 eV for $^1C_{60}^*$>).[14] ΔG_S refers to the static energy that was calculated by either $-\Delta G_S = e^2/(4\pi\epsilon_0\epsilon_R R_{CC})$ in DMF or $-\Delta G_S = -[e^2/(4\pi\epsilon_0)][1/(2R_+) + 1/(2R_-) - (1/R_{CC})/\epsilon_S - (1/(2R_+) + 1/(2R_-))/\epsilon_R]$ in toluene, where R_+ and R_- are the radii of the DPAF-C_9 radical cation (7.7 Å) and C_{60}> radical anion (4.2 Å), respectively; R_{CC} is the center−center distance between C_{60}> and DPAF-C_9 (12 Å), which were evaluated from the optimized structure; and ϵ_R and ϵ_S refer to the solvent dielectric constants for electrochemistry and photophysical measurements, respectively. The calculation of k_{CS} and Φ_{CS} was made via $^1C_{60}^*$> by the relations $k_{CS} = (1/\tau_f) - (1/\tau_{f0})$ and $\Phi_{CS} = k_{CS}/(1/\tau_f)$.

(R_+) and C_{60}> (R_-) were found to be 7.7 and 4.2 Å, respectively. The center−center distance (R_{CC}) between C_{60}> and DPAF-C_9 moieties was calculated to be 12 Å. A majority of the electron density of the HOMO was found to be localized at the DPAF-C_9 moiety, whereas the LUMO was localized mainly on the C_{60} cage moiety, suggesting the charge-separated state is $C_{60}^{\bullet-}$(>DPAF$^{\bullet+}$-C_9).

Conclusive evidence on the charge-separation and charge-recombination processes of C_{60}(>DPAF-C_9)$_n$ samples were obtained from nanosecond transient absorption measurements. The photoexcitation step was intended predominantly for the C_{60}> cage moiety with a laser light source operated at 355 nm, where the optical absorption ratio of C_{60}>/CH_3(DPAF-C_9) is nearly 87/13. This ratio may be changed as the partition of the DPAF-C_9 moiety increases in the structure of starburst multi-adducts. Because the optical absorption intensity of CH_3(DPAF-C_9) at 355 nm is at a minimum level (Figure 3a), we therefore assumed that the initial photoexcitation should transform **1** to $^1C_{60}^*$(>DPAF-C_9) as the main corresponding transient excited state. Consequently, the transient spectrum of **1** in Ar-saturated toluene taken on a time scale of 100 ns after laser light excitation exhibited the characteristic primary absorption band of the $^3C_{60}^*$> moiety centered at 700 nm (Figure 5a).[1e,14−16] The decay of the $^3C_{60}^*$> absorption profile was found to be very slow, on a time scale of 34 μs, suggesting that the intersystem crossing process going from $^1C_{60}^*$(>DPAF-C_9) to $^3C_{60}^*$(>DPAF-C_9) is the predominant event in toluene without the occurrence of competitive charge-separation events. This observation can be rationalized by the positive ΔG_{CS} values via $^1C_{60}^*$(>DPAF-C_2)$_n$ in toluene. These considerations are also supported by the high fluorescence intensity and long fluorescence lifetimes of 1.52, 1.45, and 1.50 ns for the $^1C_{60}^*$> moiety of **1**, **2**, and **3a**, respectively, in toluene.

In Ar-saturated polar DMF, a large change in the transient spectrum profiles from those taken in toluene was detected by laser light excitation at 355 nm, as shown in Figures 5b and 5c. For example, the spectrum of C_{60}(>DPAF-C_9) collected on a time scale of 100 ns after excitation by a laser pulse exhibited four absorption bands, including the first band at 700−750 nm for the ^{3}DPAF*-C_9 moiety, the second band at 700 nm for the $^3C_{60}^*$> moiety, and two other characteristic bands at 840 and 1010 nm corresponding to the absorption of DPAF$^{\bullet+}$-C_9 and $C_{60}^{\bullet-}$> transient moieties, respectively, as shown in Figure 5b.[10,15,16] Similar spectral bands were obtained for the samples of **3a** in Ar-saturated DMF, as depicted in Figure 5c. By comparison among these three figures, it is notable that the broad band centered at 740 nm, assigned for the transient absorption of the ^{3}DPAF*-C_9 moiety, apparently increased with increasing DPAF-C_9 subunits from the samples of **1** and **2** to **3a**. The characteristic band at 1010 nm, arising from the absorption of the $C_{60}^{\bullet-}$> moiety, was employed to determine the rate constants of the charge-recombination processes (k_{CR}) of $C_{60}^{\bullet-}$(>DPAF$^{\bullet+}$-C_9)(>DPAF-C_9)$_{n-1}$. This approach is reasonable because the absorption time profile in the longest wavelength region may not be disturbed by the absorption tails of $^3C_{60}^*$> and ^{3}DPAF*-C_9 moieties. As a result, the decay of its time profile (inset of Figure 5b) was well-fitted by a single-exponential function, from which the k_{CR} value was evaluated to be 6.6×10^6 s^{-1} for **1**. This k_{CR} value is comparable with that previously reported for C_{60}(>DPAF-C_2) in DMF.[10] Interestingly, the k_{CR} value became slower with the increasing number of DPAF-C_9 subunits, i.e., **1** >> **2** (1.60×10^6 s^{-1}) > **3a** (1.10×10^6 s^{-1}), as listed in Table 1. From the k_{CR} values, the lifetimes of radical ion-pairs (τ_{RIP}) were evaluated to be 150, 620, and 900 ns for $C_{60}^{\bullet-}$(>DPAF$^{\bullet+}$-C_9), $C_{60}^{\bullet-}$(>DPAF$^{\bullet+}$-C_9)(>DPAF-C_9), and $C_{60}^{\bullet-}$(>DPAF$^{\bullet+}$-C_9)(>DPAF-C_9)$_3$, respectively. From these findings, the τ_{RIP} value of the **3a** sample is ca 6.0 times longer than that of **1**, reflecting the important role of starburst DPAF-C_9 pendants that encapsulate the central C_{60} core on prolonging the lifetime of radical ion-pairs. The reason for the prolonged lifetime could simply be due to (1) the migration of the positive charge among multiple DPAF-C_9 moieties of $C_{60}^{\bullet-}$(>DPAF$^{\bullet+}$-C_9)(>DPAF-C_9)$_{n-1}$ holding up charge-recombination and (2) the starburst pentad structure preventing intermolecular aggregation, as concluded in the recent report.[12]

On the basis of the analysis of all spectroscopic transient absorption data, Figure 6 illustrates an energy level diagram that concludes all observed photoinduced events on the samples of C_{60}(>DPAF-C_9)$_n$ in DMF. We proposed that the fluorescence quenching pathway proceeded mainly through photoinduced charge-separation from the covalently bound DPAF-C_9 donor moiety to the $^1C_{60}^*$> acceptor moiety leading to the formation of $C_{60}^{\bullet-}$(>DPAF$^{\bullet+}$-C_9)(>DPAF-C_9)$_{n-1}$ transient state. Subsequent charge-recombination of the radical ion pairs returns **1**−**3a** directly back to their ground state.

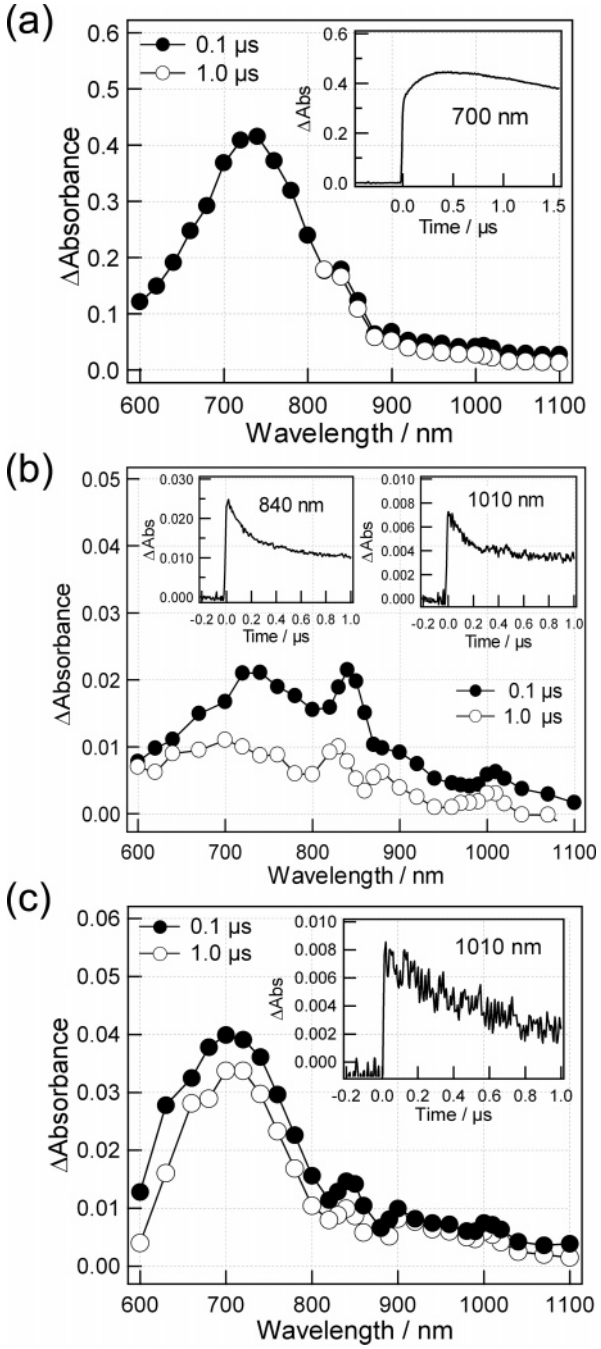

Figure 5. Nanosecond transient spectra of (a) **1** in toluene, (b) **1** in DMF, and (c) **3a** in DMF, obtained by laser light excitation at 355 nm. The inset shows the time profiles.

Conclusion

Attachment of four hindered C_9 groups in the structure of starburst **3** largely improves the solubility, the ability to enhance molecular dispersion in the solvents, and the possibility to inhibit direct intermolecular stacking and contact among fullerene cages and diphenylaminodialkylfluorene rings. Accordingly, high quantum yields (Φ_{CS}) of the charge-separation process via $^1C_{60}^*(>\text{DPAF-C}_9)_n$ in the range 0.83−0.90 were obtained for the formation of $C_{60}^{\bullet-}(>\text{DPAF}^{\bullet+}\text{-C}_9)(>\text{DPAF-C}_9)_{n-1}$. The results indicated their good photoquantum efficiency in charge generation in DMF. Interestingly, τ_{RIP} was found to be 900 ns for **3a**, which is 6-fold longer than that of its linear analogue **1**. It implied the important role of sterically clouded DPAF-C_9 pendants, arranged in a starburst environment that encapsulates the central C_{60} core, on extending the lifetime of radical ion-pairs. We interpreted these phenomena by the intramolecular migration or exchange of a positive charge among multiple DPAF-C_9 subunits of $C_{60}^{\bullet-}(>\text{DPAF}^{\bullet+}\text{-C}_9)(>\text{DPAF-C}_9)_{n-1}$ that becomes responsible for the delay of charge-recombination. Because fast, efficient charge-generation and long-lived charge-separation states between donor and acceptor components are known to be critical factors for the design of photovoltaic cells, the present use of starburst $C_{60}-(\text{donor})_x$ covalent conjugates may lead to a better understanding of their structural relationship to the efficiency of photodevices.

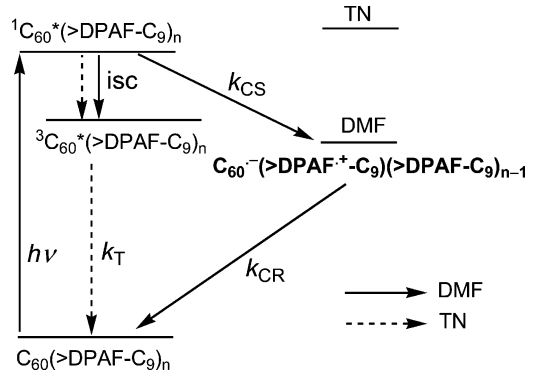

Figure 6. Energy level diagram of $C_{60}(>\text{DPAF-C}_9)_n$ in DMF and toluene (TN), showing a charge-separated state $C_{60}^{\bullet-}(>\text{DPAF}^{\bullet+}\text{-C}_9)(>\text{DPAF-C}_9)_{n-1}$.

Acknowledgment. The authors at UML are thankful for the financial support of the Air Force Office of Scientific Research, under contract No. FA9550-05-1-0154, and the Air Force Research Laboratory, under contract No. FA8601-07-P-0068. The present work was also partly supported by a Grant-in-Aid on Scientific Research of Priority Area (417) from the Ministry of Education, Science, Sports, and Culture of Japan.

Supporting Information Available: Synthetic procedures of $C_{60}(>\text{DPAF-C}_9)_n$ with MALDI-TOF mass spectrum of the tetraadduct $C_{60}(>\text{DPAF-C}_9)_4$ **3b** (Figure S1), steady-state fluorescence spectra of $C_{60}(>\text{DPAF-C}_9)_n$ in toluene and DMF (Figure S2), fluorescence decay profiles of $C_{60}(>\text{DPAF-C}_9)_n$ in DMF (Figure S3), and calculated HOMO and LUMO of **1** (Figure S4). These materials are available free of charge via the Internet at http://pubs.acs.org.

References and Notes

(1) (a) Guldi, D. M.; Kamat, P. V. *Fullerenes, Chemistry, Physics and Technology*; Kadish, K. M., Ruoff, R. S., Eds.; Wiely-Interscience: New York, 2000; pp 225−281. (b) Maggini, M.; Guldi, D. M. *Molecular and Supramolecular Photochemistry*; Ramamurthy, V., Schanze, K. S., Eds.; Marcel Dekker: New York, 2000; Vol. 4, pp 149−196. (c) Martin, N.; Sanchez, L.; Illescas, B.; Perez, I. *Chem. Rev.* **1998**, *98*, 2527−2548. (d) Prato, M.; Maggini, M. *Acc. Chem. Res.* **1998**, *31*, 519−530. (d) Diederich, F.; Gomez-Lopez, M. *Chem. Soc. Rev.* **1999**, *28*, 263−277. (e) For a review on fullerene excited states see Guldi, D. M.; Prato, M. *Acc. Chem. Res.* **2000**, *33*, 695−703. (f) Guldi, D. M. *Chem. Soc. Rev.* **2002**, *31*, 22−36. (g) El-Khouly, M. E.; Ito, O.; Smith, P. M.; D'Souza, F. *J. Photochem. Photobiol., C* **2004**, *5*, 79−104.

(2) (a) Imahori, H.; Sakata, Y. *Eur. J. Org. Chem.* **1999**, 2445−2457. (b) Jolliffe, K. A.; Langford, S. J.; Ranasinghe, M. G.; Shephard, M. J.; Paddon-Row, M. N. *J. Org. Chem.* **1999**, *64*, 1238−1246. (c) Liu, S.-G.; Shu, L.; Rievera, J.; Liu, H.; Raimundo, J.-M.; Roncali, J.; Gorgues, A.; Echegoyen, L. *J. Org. Chem.* **1999**, *64*, 4884−4886. (d) Hutchison, K.; Gao, J.; Schick, G.; Rubin, Y.; Wudl, F. *J. Am. Chem. Soc.* **1999**, *121*, 5611−5612. (e) Nierengarten, J.-F.; Eckert, J.-F.; Nicoud, J.-F.; Ouali, L.; Krasnikov, V.; Hadziioannou, G. *Chem. Commun.* **1999**, 617−618. (f) Imahori, H.; Azuma, T.; Ozawa, S.; Yamada, H.; Ushida, K.; Ajavakom, A.; Norieda, H.; Sakata, Y. *Chem. Commun.* **1999**, 557−558. (g) Guldi, D. M.; Luo, C.; Ros, T. D.; Prato, M.; Dietel, E.; Hirsch, A. *Chem. Commun.* **2000**, 375−376. (h) Roman, L. S.; Inganas, O.; Granlund, T.; Nyberg, T.;

Svensson, M.; Andersson, M. R.; Hummelen, J. C. *Adv. Mater*. **2000**, *12*, 189−195. (i) Van Hal, P. A.; Beckers, E. H. A.; Meskers, S. C. J.; Janssen, R. A. J.; Jousselme, B.; Blanchard, P.; Roncali, J. *Chem.—Eur. J*. **2002**, *8*, 5415−5429.

(3) (a) Sariciftci, N. S.; Smilowitz, L.; Heeger, A. J.; Wudl, F. *Science* **1992**, *258*, 1474−1476. (b) Sariciftci, N. S.; Braun, D.; Zhang, C.; Srdanov, V. I.; Heeger, A. J.; Stucky, G.; Wudl, F. *Appl. Phys. Lett*. **1993**, *62*, 585−587. (c) Yu, G.; Gao, J.; Hummelen, J. C.; Wudl, F.; Heeger, A. J. *Science* **1995**, *270*, 1789−1791. (d) Halls, J. J. M.; Pichler, K.; Friend, R. H.; Moratti, S. C.; Holmes, A. B. *Appl. Phys. Lett.* **1996**, *68*, 3120−3122. (e) Mattoussi, H.; Rubner, M. F.; Zhou, F.; Kumar, J.; Tripathy, S. K.; Chiang, L. Y. *Appl. Phys. Lett.* **2000**, *77*, 1540−1542. (f) Brabec, C. J.; Sariciftci, N. S.; Hummelen, J. C. *Adv. Funct. Mater*. **2001**, *11*, 15−26. (g) Yamada, H.; Imahori, H.; Nishimura, Y.; Yamazaki, I.; Ahn, T. K.; Kim, S. K.; Kim, D.; Fukuzumi, S. *J. Am. Chem. Soc*. **2003**, *125*, 9129−9139. (h) Segura, J. L.; Martin, N.; Guldi, D. M. *Chem. Soc. Rev*. **2005**, *34*, 31−47. (i) Roncali, J. *Chem. Soc. Rev*. **2005**, *34*, 483−495.

(4) (a) Sera, N.; Tokiwa, H.; Miyata, N. *Carcinogenesis* **1996**, *17*, 2163−2169. (b) Irie, K.; Nakamura, Y.; Ohigashi, H.; Tokuyama, H.; Yamago, S.; Nakamura, E. *Biosci., Biotechnol., Biochem*. **1996**, *60*, 1359−1361. (c) Yu, C.; Canteenwala, T.; Chen, H. H. C.; Chen, B. J.; Canteenwala, M.; Chiang, L. Y. *Proc. − Electrochem. Soc*. **1999**, *99−12*, 234−249. (d) Hirayama, J.; Abe, H.; Kamo, N.; Shinbo, T.; Ohnishi-Yamada, Y.; Kurosawa, S.; Ikebuchi, K.; Sekiguchi, S. *Biol. Pharm. Bull*. **1999**, *22*, 1106−1109. (e) Yu, C.; Canteenwala, T.; Chen, H. C.; Jeng, U. S.; Lin, T. L.; Chiang, L. Y. Free Radical Scavenging and Photodynamic Functions of Micelle-like Hydrophilic Hexa(sulfobutyl)fullerene (FC_4S) In *Perspectives of Fullerene Nanotechnology*; Osawa, E., Ed.; Kluwer Academic Publisher: Great Britian, 2002; pp 165−183. (f) Nakanishi, I.; Fukuzuami, S.; Konishi, T.; Ohkubo, K.; Fujitsuka, M.; Ito, O.; Miyata, N. *J. Phys. Chem. B* **2002**, *106*, 2372−2380. (g) Nakamura, E.; Isobe, H. *Acc. Chem. Res*. **2004**, *36*, 807−815. (h) Yu, C.; Canteenwala, T.; El-Khouly, M. E.; Araki, Y.; Chiang, L. Y.; Wilson, B. C.; Ito, O.; Pritzker, K. *J. Mater. Chem.* **2005**, *15*, 1857−1864.

(5) (a) Chiang, L. Y.; Padmawar, P. A.; Canteenwala, T.; Tan, L.-S.; He, G. S.; Kannan, R.; Vaia, R.; Lin, T.-C.; Zheng, Q.; Prasad, P. N. *Chem. Comm*. **2002**, 1854−1855. (b) Padmawar, P. A.; Canteenwala, T.; Verma, S.; Tan, L.-S.; He, G. S.; Prasad, P. N.; Chiang, L. Y. *Synth. Met*. **2005**, *154*, 185−188.

(6) Tanihara, J.; Ogawa, K.; Kobuke, Y. *J. Photochem. Photobiol., A* **2006**, *178*, 140−149.

(7) (a) He, G. S.; Bhawalkar, J. D.; Zhao, C. F.; Prasad, P. N. *Appl. Phys. Lett*. **1995**, *67*, 2433−2435. (b) Ehrlich, J. E.; Wu, X. L.; Lee, L.-Y.; Hu, Z.-Y.; Roeckel, H.; Marder, S. R.; Perry, J. W. *Opt. Lett*. **1997**, *22*, 1843−1845. (c) Silly, M. G.; Porres, L.; Mongin, O.; Chollet, P.-A.; Blanchard-Desce, M. *Chem. Phys. Lett*. **2003**, *379*, 74−80.

(8) (a) Padmawar, P. A.; Canteenwala, T.; Tan, L.-S.; Chiang, L. Y. *J. Mater. Chem*. **2006**, *16*, 1366−1378. (b) Padmawar, P. A.; Canteenwala, T.; Verma, S.; Tan, L.-S.; Chiang, L. Y. *J. Macromol. Sci., Pure Appl. Chem*. **2004**, *41*, 1387−1400.

(9) Padmawar, P. A.; Rogers, J. O.; He, G. S.; Chiang, L. Y.; Canteenwala, T.; Tan, L.-S.; Zheng, Q.; Lu, C.; Slagle, J. E.; Danilov, E.; McLean, D. G.; Fleitz, P. A.; Prasad, P. N. *Chem. Mater*. **2006**, *18*, 4065−4074.

(10) Luo, H.; Fujitsuka, M.; Ito, O.; Padmawar, P.; Chiang, L. Y. *J. Phys. Chem. B*. **2003**, *107*, 9312−9318.

(11) Verma, S.; Hauck, T.; El-Khouly, M. E.; Padmawar, P. A.; Canteenwala, T.; Pritzker, K.; Ito, O.; Chiang, L. Y. *Langmuir* **2005**, *21*, 3267−3272.

(12) Elim, H. I.; Anandakathir, R.; Jakubiak, R.; Chiang, L. Y.; Ji, W.; Tan, L. S. *J. Mater. Chem*. **2007**, *17*, 1826−1838.

(13) (a) Rehm, D.; Weller, A. *Ber. Bunsen−Ges* **1969**, *73*, 834−839. (b) Weller, A. *Z. Phys. Chem. Neue Folge* **1982**, *133*, 93−98.

(14) Foote, C. S. *Top. Curr. Chem*. **1994**, *169*, 347−363.

(15) (a) Guldi, D. M. *Chem. Commun*. **2000**, 321−327. (b) Reed, C. A.; Bolskar, R. D. *Chem. Rev*. **2000**, *100*, 1075−1120. (c) Gust, D.; Moore, T. A.; Moore, A. L. *J. Photochem. Photobiol., B* **2000**, *58*, 63−71. (d) Imahori, H.; El-Khouly, M. E.; Fujitsuka, M.; Ito, O.; Sakata, Y.; Fukuzumi, S. *J. Phys. Chem. A* **2001**, *105*, 325−332.

(16) (a) D'Souza, F.; Deviprasad, G. R.; El-Khouly, M. E.; Fujitsuka, M.; Ito, O. *J. Am. Chem. Soc*. **2001**, *123*, 5277−5284. (b) El-Khouly, M. E.; Araki, Y.; Ito, O.; Gadde, S.; McCarty, A. L.; Karr, P. A.; Zandler, M. E.; D'Souza, F. *Phys. Chem. Chem. Phys*. **2005**, *7*, 3163−3171. (c) El-Khouly, M. E.; Padmawar, P.; Araki, Y.; Verma, S.; Chiang, L. Y.; Ito, O. *J. Phys. Chem. A* **2006**, *110*, 884−891.